

## Microwave Assisted Synthesis of Titanium(IV) Doped Hydroxyapatite and its Antibacterial Activities

A. JENIFER<sup>1</sup>, P. SAKTHIVEL<sup>1,\*</sup>, K. SENTHILARASAN<sup>2</sup>, S. ARUMUGAM<sup>3</sup> and P. SIVAPRAKASH<sup>3</sup>

<sup>1</sup>P.G. and Research Department of Physics, Urumu Dhanalakshmi College, Tiruchirappalli-621819, India

<sup>2</sup>P.G. and Research Department of Physics, Edayathangudy G.S. Pillay Arts and Science College, Nagapattinam-611002, India

<sup>3</sup>Centre for High Pressure Research, School of Physics, Bharathidasan University, Tiruchirappalli-620024, India

\*Corresponding author: E-mail: sakthiphy13@gmail.com

Received: 16 August 2019;

Accepted: 1 October 2019;

Published online: 30 December 2019;

AJC-19726

A rapid, efficient and cost-effective method for the synthesis of titanium(IV) doped hydroxyapatite using microwave assisted wet chemical method is reported. The synthesized hydroxyapatite and titanium(IV) doped hydroxyapatite (THA) samples were characterized by using XRD, FTIR and HR-TEM with EDAX. The antibacterial activity against *Staphylococcus aureus* and *Escherichia coli* was investigated by using the disc diffusion method showed good results. The anti-inflammatory activity by using the protein denaturation method proves to be less inflammable for *in vivo* applications. The hemolytic test showed that the samples are less hemolytic.

**Keywords:** Hydroxyapatite, Titanium dioxide, Wet chemical method, Antibacterial effect, Anti-inflammatory, Hemolytic studies.

### INTRODUCTION

Bone matrix is precisely composed of two major phases at the nanoscale level namely, organic (protein) and inorganic (mineral) which resembles as nanocomposites [1,2]. Hydroxyapatite  $[\text{Ca}_{10}(\text{PO}_4)_6\text{OH}_2]$  is close to the apatite structure and composition of bone mineral with the diverse properties of bioactivity, biocompatibility and osteoconduction [3]. The structure of hydroxyapatite in bone mineral is in the form of nanocrystals with dimensions of about 4 nm × 50 nm × 50 nm. The stoichiometric ratio of Ca/P is 1.67 with the structure of hydroxyapatite is well recognized for ionic substitution [4]. The incorporation of metal oxides leads to study the tailoring properties of synthetic hydroxyapatite. The non-toxic material is used in various applications like bone implantation, drug delivery system and water catalyst management [5,6]. The absence of antibacterial property in synthetic hydroxyapatite results in the presence of bacteria in bioimplants which results in the formation of infections in the implanted surroundings. Hydroxyapatite modified with metal ions such as Zn, Mg, Cu, Ag, Ni and Ti exists to prevail these problems [7-9]. Titanium(IV) ions which are non-existent in the human body by nature are used for bone implants and

catalyst due to its properties similar to natural bone [10]. The non-existence of data regarding the cytotoxicity of titanium(IV) doped hydroxyapatite (THA) on human body cells proves the application of titanium in bio implants [8]. Besides the applications of THA in orthopaedics and dental surgery, it has been corroborated the outcome of photo-catalyst effect of THA promotes in blood purifying therapies [11].

Techniques for the synthesis of ion incorporated hydroxyapatite reported till date includes wet chemical [12], sol-gel [13], hydrothermal [14], microwave methods [15]. Among these techniques, microwave-assisted technique is used for the preparation of inorganic nanostructure materials which are rapid, convenient and efficient [14]. The aim of this work is to synthesize titanium doped hydroxyapatite (THA) nanoparticles with properties similar to that of natural bone in the stoichiometric ratio 1.67 and investigation of its antibacterial efficacy. The THA nanoparticles is prepared by microwave assisted wet-chemical method which is less time consuming and cost effective. The synthesized samples were characterized by using XRD, FTIR, HRTEM, EDAX and *in vitro* studies in which the antibacterial, anti-inflammatory activities and hemolytic property of the samples was studied.

## EXPERIMENTAL

The synthesis of hydroxyapatite and Ti(IV) doped hydroxyapatite (THA) nanoparticles was performed *via* microwave-assisted wet chemical method by using calcium hydroxide [Ca(OH)<sub>2</sub>, Merck], ammonium dihydrogen phosphate (NH<sub>4</sub>H<sub>2</sub>PO<sub>4</sub>, Merck), titanium dioxide (TiO<sub>2</sub>, Merck) as the starting precursors. Solution of 1 M Ca(OH)<sub>2</sub> and 0.6 M NH<sub>4</sub>H<sub>2</sub>PO<sub>4</sub> were dissolved in separate 100 mL distilled water. Then, 0.2 M of TiO<sub>2</sub> was added to calcium precursor solution and stirred vigorously for 1 h. Ammonium dihydrogen phosphate solution was added dropwise to Ca(OH)<sub>2</sub> solution for about 30 min. The mixed solution was stirred continuously and the pH maintained above 10 and subjected to microwave irradiation for 20 min. The resultant precipitate was washed thrice to remove the presence of excess ammonia. The filtered solution was dried and calcinated at 900 °C for 2 h. The obtained flakes were grained to a fine powder by using a mortar and pestle. The synthesis of hydroxyapatite nanopowder was prepared without the addition of TiO<sub>2</sub> into calcium precursor.

**Characterization:** The phase analysis for the synthesized samples was analyzed by using X-ray diffractometer Smartlab Rigaku operated at 40 kV and 30 mA with Cu K $\alpha$  radiation in the range from 5° to 80° in continuous mode. The scan speed or duration is 4.06 °/min. The structural transformation was analyzed by using Perkin-Elmer spectrometer. The morphology and particle size of sample were analyzed by using high resolution transmission electron microscope (TECNAI, G20 TWIN) at 200 keV.

**Antibacterial assay:** The antibacterial activity of hydroxyapatite and titanium(IV) doped hydroxyapatite (THA) samples were investigated by using disc diffusion method [16]. Petri plates were prepared by pouring 30 mL of nutrient agar medium for bacteria. The test organism was inoculated on a solidified agar plate with the help of micropipette and spread and allowed to dry for 10 min. The surfaces of media were inoculated with bacteria from a broth culture. A sterile cotton swab is dipped into a standardized bacterial test suspension and used to evenly inoculate the entire surface of nutrient agar plate. Briefly, inoculums containing Gram-positive bacteria *Staphylococcus aureus* (MTCC 3160) and Gram-negative bacteria *Escherichia coli* (MTCC 732) were spread on nutrient agar plates separately. Using sterile forceps, the sterile filter papers (6 mm diameter) containing the crude extracts (50, 100 and 150  $\mu$ L) were laid down on the surface of inoculated agar plate. The plates were incubated at 37 °C for 24 h for bacteria and at room temperature (30  $\pm$  1 °C). Each sample was tested in triplicate. The antimicrobial potential of test compounds was determined on the basis of the mean diameter of zone of inhibition around the disc in millimeters.

**Anti-inflammatory activity:** Anti-inflammatory activity was assessed by using the protein denaturation method [17]. The reaction mixture (5 mL) consisting of 2 mL of different concentrations of hydroxyapatite and titanium(IV) doped hydroxyapatite (THA) (100, 200, 300, 400 and 500  $\mu$ g/mL) and 2.8 mL of phosphate buffered saline (pH 6.4) was mixed with 0.2 mL of egg albumin (fresh hen's egg) and incubated at 37  $\pm$  1 °C for 15 min. Denaturation was induced by keeping

the reaction mixture at 70 °C in a water bath for 10 min. After cooling, the absorbance was measured at 660 nm by using double distilled water as a blank. Diclofenac sodium (100, 200, 300, 400 and 500  $\mu$ g/mL) is used as standard drug and similarly for determination of absorbance. Both samples were done in triplicate and the average was taken. The percentage inhibition of protein denaturation was calculated as follows:

$$\text{Inhibition (\%)} = \frac{A_t - A_c}{A_c} \times 100$$

where, A<sub>t</sub> = absorbance of the test sample; A<sub>c</sub> = absorbance of control.

**Hemolysis test:** *in vitro* Hemolytic activity was performed by spectrophotometer method [18]. Fresh human blood (5 mL) was collected in a tube containing heparin. Institutional Review Board approval was obtained. The blood was centrifuged at 1500 rpm and plasma (supernatant) was discarded. The pellet was washed with sterile phosphate buffer saline solution (pH 7.2  $\pm$  0.2) by centrifugation at 1500 rpm for 5 min. The cell suspension was prepared by finally diluting the pellet to 0.5% in saline solution. 0.5 mL of the cell suspension was mixed with 0.5 mL of the samples (25, 50, 100, 250, and 500  $\mu$ g/mL concentrations in phosphate buffer saline). The mixtures were incubated for 30 min at 37 °C and centrifuged at 1500 rpm for 10 min. The free hemoglobin in the supernatant was measured in UV-Vis spectrophotometer at 412 nm. Phosphate buffer saline and distilled water were used as minimal and maximal hemolytic controls. Each sample was performed in triplicates at each concentration. The level of percentage hemolysis by the sample was calculated as follows:

$$\text{Hemolysis (\%)} = \frac{A_t - A_n}{A_c - A_n} \times 100$$

where A<sub>t</sub> is the absorbance of the test sample, A<sub>n</sub> is the absorbance of the negative control (saline control) and A<sub>c</sub> is the absorbance of positive control (water control). The hemolysis level is > 5, 2-5 and 0-2, the corresponding hemolytic grade is hemolytic, slightly hemolytic and non-hemolytic, respectively.

## RESULTS AND DISCUSSION

**XRD analysis:** The XRD patterns for the synthesized samples are given in Fig. 1. The characteristic peaks in both hydroxyapatite and titanium(IV) doped hydroxyapatite (THA) in the regions 25°, 28°, 31-34° and 48-56° is agreeable with the JCPDS card: 09-0432 of hexagonal hydroxyapatite. In THA pattern, there is a slight shifting of peak positions from higher value to lower value and decrease in the intensity of characteristic peaks is due to the substitution of Ti ions (0.605 Å) instead of Ca ions (0.99 Å) in the hydroxyapatite structure. The grain size was calculated by using Debye-Scherrer formula and the size of hydroxyapatite and THA nanoparticles are found to be 55 and 49 nm, respectively. The reduction in crystallite size is due to the contraction of hydroxyapatite matrix as the result of incorporation of Ti ions into the sites of calcium ions [19].

**FTIR analysis:** The FTIR spectrum with wavelength ranging from 4000 to 400 cm<sup>-1</sup> for hydroxyapatite and THA samples is shown in Fig. 2. The key IR bands of functional groups of the samples are given in Table-1. The spectra show

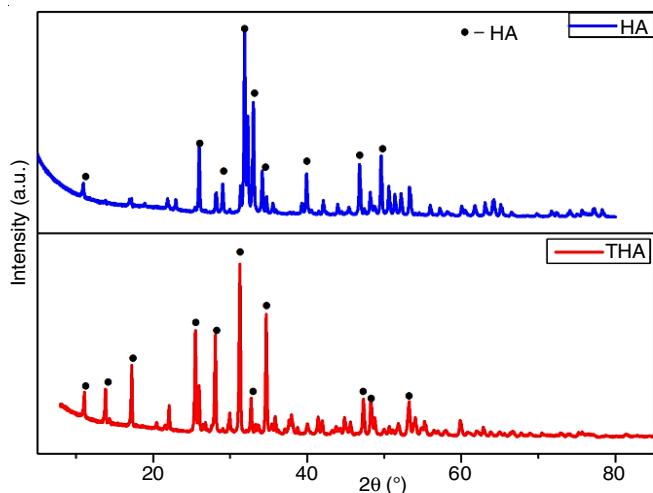


Fig. 1. XRD spectra of hydroxyapatite (HA) and THA nanopowder calcinated at 900 °C for 2 h

the bands of OH group stretching and libration at 3574 and 634  $\text{cm}^{-1}$  [20,21]. The presence of  $\text{PO}_4^{3-}$  group is confirmed by the absorption peaks between 1094 and 964  $\text{cm}^{-1}$  with P-O stretching vibration and O-P-O bending vibration between 603 and 572  $\text{cm}^{-1}$ . In case of THA, the incorporation of  $\text{Ti}^{2+}$  in hydroxyapatite structure is confirmed by the dehydroxylation

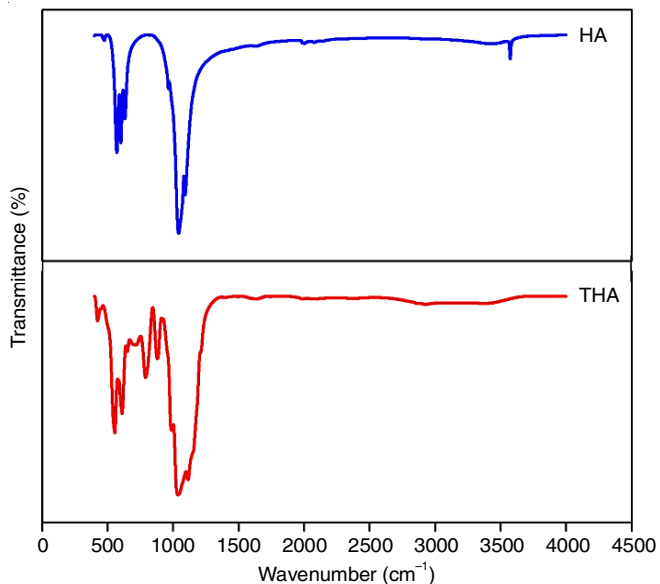


Fig. 2. FTIR spectra ( $\text{cm}^{-1}$ ) of hydroxyapatite (HA) and THA powders calcinated at 900 °C

TABLE-1  
OBSERVED TRANSMITTANCE PEAKS IN THE  
FTIR SPECTRA OF HYDROXYAPATITE AND  
THA POWDERS CALCINATED AT 900 °C

Hydroxyapatite	THA	Vibrational mode	Functional group
472	429	$\nu_2$	$\text{PO}_4^{3-}$
574, 605	556, 607	$\nu_4$	$\text{PO}_4^{3-}$
635	795, 735	Libration	$\text{OH}^-$
	879	$\nu_3$	$\text{CO}_3^{2-}$
996	990	$\nu_1$	$\text{PO}_4^{3-}$
1044, 1097	1046, 1118	$\nu_3$	$\text{PO}_4^{3-}$
3415	3429		$\text{H}_2\text{O}$
3574			$\text{OH}^-$

of OH group at 3574 and 634  $\text{cm}^{-1}$ , libration of OH group at 784  $\text{cm}^{-1}$ . The broadening of  $\text{PO}_4^{3-}$  peak between 990 and 1106  $\text{cm}^{-1}$  is due to the presence of Ti ions in hydroxyapatite lattice. The calcination of samples at 900 °C substantially reduced the presence of  $\text{CO}_3^{2-}$  ions and clearly visible in the spectrum with strong depletion in the  $\text{CO}_2$  bands intensity [21].

The presence of  $\text{CO}_3^{2-}$  at 874  $\text{cm}^{-1}$  in the THA spectrum is due to the incorporation of Ti ions in place of Ca ions [20]. The absence of peak at 3737  $\text{cm}^{-1}$  confirms the deformation of Ti-OH in the surface of Ti-HA sample which occurs due to the dislocation of OH group, however, the reason for the dislocation is still unclear [10].

**HRTEM and EDAX analysis:** The HRTEM images of hydroxyapatite and THA nanopowder is shown in Fig. 3. Both hydroxyapatite and THA nanoparticles resemble spherical like morphology with agglomeration due to calcination at 900 °C. The presence of porosity in hydroxyapatite confirms the similarity of natural bone mineral. The reduction of porosity in the THA nanoparticles proves the incorporation of Ti ions into the hydroxyapatite structure [22-24].

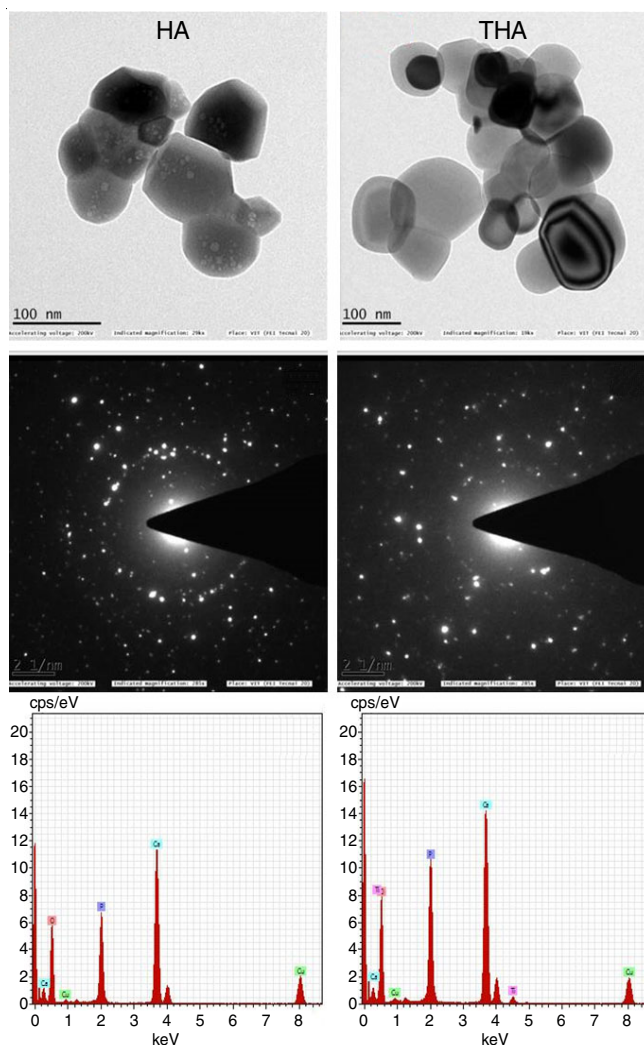


Fig. 3. HRTEM, SAED pattern and EDAX images of hydroxyapatite (HA) and THA

The SAED pattern resembles the crystallinity of samples with sporadic diffraction which confirms with the XRD pattern.

The EDAX spectra displays the detection of Ti, Ca, P, O in THA sample. The Ca/P ratio of hydroxyapatite sample is  $1.69 \pm 0.02$  and THA is  $1.83 \pm 0.03$ . The incorporation of Ti in the hydroxyapatite structure increased the Ca/P ratio to 0.14. In hydroxyapatite and THA samples, concentration of phosphorus remained nearly constant regardless of the doping element. In contrast, amount of calcium decreases in the dopant samples, indicating the replacement of calcium by doping element.

**Antibacterial activity:** Antibacterial activity for hydroxyapatite and THA nanoparticles against *Staphylococcus aureus* and *Escherichia coli* was investigated by using the disc diffusion method. The lysis zone extended to approximately 0.2 cm for the concentration of 150 mL was observed after incubation for 24 h. The THA sample shows better effectiveness than hydroxyapatite against *Escherichia coli* (Fig. 4). The *E. coli* bacterium which causes major infection by means of surgical instrument or implantation can be solved by using materials containing properties with antibacterial effect [9]. Hydroxyapatite, which is naturally bioactive and biocompatible generally does not have antibacterial property [25]. This can be developed by using  $Ti^{2+}$  ions incorporation in the hydroxyapatite structure which shows efficacy against the common pathogens *S. aureus* and *E. coli* [26].

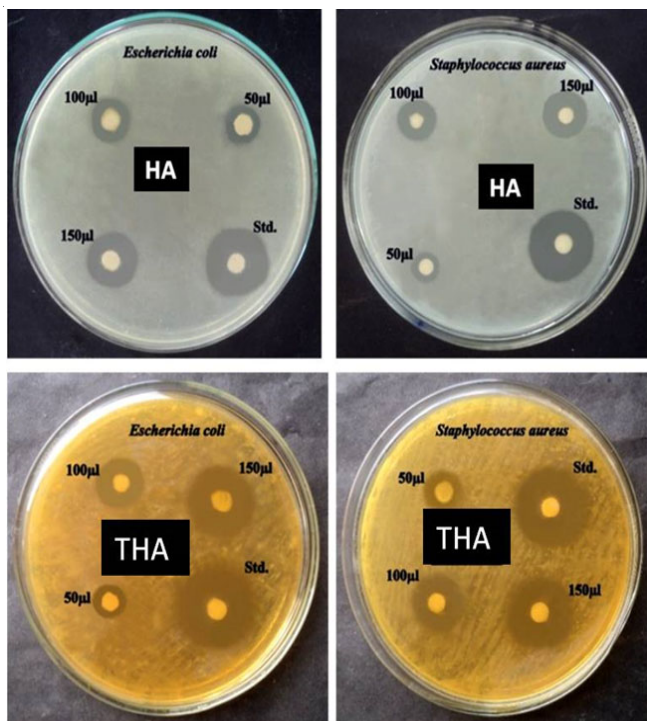


Fig. 4. Antibacterial activity of hydroxyapatite and THA samples against Gram-positive and Gram-negative bacteria *S. aureus* and *E. coli*

**Anti-inflammatory activity:** Anti-inflammatory activity of hydroxyapatite and THA samples by using diclofenac sodium as standard drug for absorbance is shown in Fig. 5. The percentage of inhibition for different concentrations is nearer to standard drug. The observation indicates the effectiveness of THA than pure hydroxyapatite sample. Therefore, a low concentration of  $Ti^{2+}$  in THA samples can be used for implantation oriented application, which does not cause any higher inflammation to the cellular system [27].

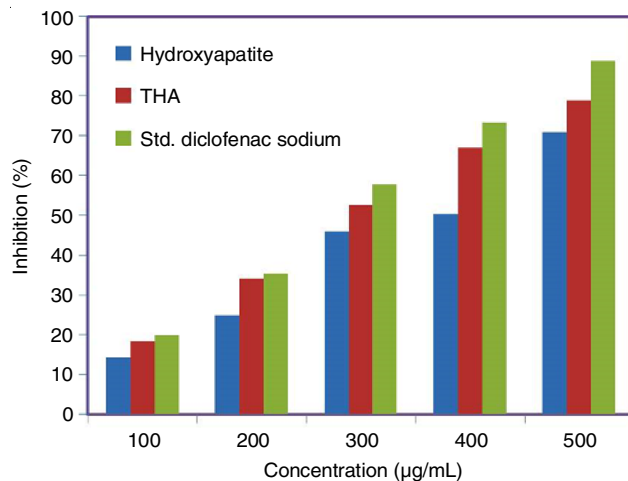


Fig. 5. Anti-inflammatory activity of hydroxyapatite and THA samples compared with the standard drug diclofenac sodium

**Hemolysis test:** The application of THA in implants and blood purifying therapies include the investigation of hemolytic property of samples, which interacts with the blood cells and other cellular systems [28]. Hemolysis test is certainly an essential test for studying the interaction of nanoparticles with blood components [29]. A human cellular system's adaption or interaction to external bodies may sometimes cause thrombus and decrease in the stimulation of platelet activation [28]. The ASTM F 756-00 states that hemolysis ratio  $< 2$  and 2-5 is considered as non-hemolytic and slightly hemolytic. Hence, hydroxyapatite and THA samples observed as slightly hemolytic (Table-2).

TABLE-2  
OD VALUES OF HEMOLYSIS TEST FOR  
HYDROXYAPATITE AND THA SAMPLES

Sample	Absorbance	Positive	Negative	Hemolysis ratio
Hydroxyapatite	0.67	1.652	0.057	0.629
THA	0.10	1.652	0.057	2.695

## Conclusion

Crystalline nanopowder with Ca/P nearby to 1.67 was synthesized via a combination of wet chemical and microwave-assisted method. The samples were categorized as hexagonal structured and crystalline with the size of 55 nm for hydroxyapatite and 49 nm for titanium(IV) doped hydroxyapatite (THA). The FTIR analysis confirmed the presence of phosphate and hydroxyl group. The HRTEM with EDAX confirms the morphology of nanoparticles as spherical and presence of elements Ca, P, O and Ti. The absence of CO in the EDAX analysis confirms the purity of prepared sample. The THA sample exhibited good anti-inflammatory activity and as less hemolytic. The antibacterial activity of THA samples against *Staphylococcus aureus* and *Escherichia coli* makes it applicable for biomedical applications.

## ACKNOWLEDGEMENTS

The authors are thankful to the Centre for High Pressure Research (CHPR), Bharathidasan University, Tiruchirappalli, India for their partial support in the research work.

### CONFLICT OF INTEREST

The authors declare that there is no conflict of interests regarding the publication of this article.

### REFERENCES

- W.J. Boyle, W.S. Simonet and D.L. Lacey, *Nature*, **423**, 337 (2003); <https://doi.org/10.1038/nature01658>.
- X. Feng, *Curr. Chem. Biol.*, **3**, 189 (2009); <https://doi.org/10.2174/187231309788166398>.
- M. Vallet-Regí and J.M. González-Calbet, *Prog. Solid State Chem.*, **32**, 1 (2004); <https://doi.org/10.1016/j.progsolidstchem.2004.07.001>.
- R. Murugan and S. Ramakrishna, *Compost. Sci. Technol.*, **65**, 2385 (2005).
- Q.L. Feng, T.N. Kim, J. Wu, E.S. Park, J.O. Kim, D.Y. Lim and F.Z. Cui, *Thin Solid Films*, **335**, 214 (1998); [https://doi.org/10.1016/S0040-6090\(98\)00956-0](https://doi.org/10.1016/S0040-6090(98)00956-0).
- T.N. Kim, Q.L. Feng, J.O. Kim, J. Wu, H. Wang, G.C. Chen and F.Z. Cui, *J. Mater. Sci. Mater. Med.*, **9**, 129 (1998); <https://doi.org/10.1023/A:1008811501734>.
- P. Sivaprakash, A.N. Ananth, V. Nagarajan, S.P. Jose and S. Arumugam, *Mater. Res. Bull.*, **95**, 17 (2017); <https://doi.org/10.1016/j.materresbull.2017.07.017>.
- S. Arumugam, P. Sivaprakash, A. Dixit, R. Chaurasiya, L. Govindaraj, M. Sathiskumar, S. Chatterjee and R. Suryanarayanan, *Sci. Rep.*, **9**, 3200 (2019); <https://doi.org/10.1038/s41598-019-39083-8>.
- N. Iqbal, M.R. Abdul Kadir, N.A.N. Nik Malek, N. Humaimi Mahmood, M. Raman Murali and T. Kamarul, *Mater. Lett.*, **89**, 118 (2012); <https://doi.org/10.1016/j.matlet.2012.08.057>.
- K. Kandori, M. Oketani, Y. Sakita and M. Wakamura, *J. Mol. Catal. Chem.*, **360**, 54 (2012); <https://doi.org/10.1016/j.molcata.2012.04.009>.
- K. Kandori, M. Oketani and M. Wakamura, *Colloids Surf. B Biointerf.*, **102**, 908 (2013); <https://doi.org/10.1016/j.colsurfb.2012.09.022>.
- M.R. Saeri, A. Afshar, M. Ghorbani, N. Ehsani and C.C. Sorrell, *Mater. Lett.*, **57**, 4064 (2003); [https://doi.org/10.1016/S0167-577X\(03\)00266-0](https://doi.org/10.1016/S0167-577X(03)00266-0).
- C.M. Mardziah, I. Sopyan and S. Ramesh, *Artif. Organs*, **23**, 105 (2009).
- V. Sarath Chandra, G. Baskar, R.V. Suganthi, K. Elayaraja, M.I. Ahymah Joshy, W. Sofi Beaula, R. Mythili, G. Venkatraman and S. Narayana Kalkura, *ACS Appl. Mater. Interfaces*, **4**, 1200 (2012); <https://doi.org/10.1021/am300140q>.
- W. Pon-On, S. Meejoo and M. Tang, *Int. J. Nanosci.*, **6**, 9 (2007); <https://doi.org/10.1142/S0219581X07004262>.
- O.A. Awoyinka, I.O. Balogun and A.A. Ogunnowo, *J. Med. Plants Res.*, **1**, 63 (2007).
- N.I. Osman, N.J. Sidik, A. Awal, N.A.M. Adam and N.I. Rezali, *J. Intercult. Ethnopharmacol.*, **5**, 343 (2016); <https://doi.org/10.5455/jice.20160731025522>.
- Z.-G. Yang, H.-X. Sun and W.-H. Fang, *Vaccine*, **23**, 5196 (2005); <https://doi.org/10.1016/j.vaccine.2005.06.016>.
- K. Arul, E. Kolanthai, E. Manikandan, G.M. Bhalerao, V.S. Chandra, J.R. Ramya, U.K. Mudali, K.G.M. Nair and S.N. Kalkura, *Mater. Res. Bull.*, **67**, 55 (2015); <https://doi.org/10.1016/j.materresbull.2015.02.054>.
- S. Meejoo, W. Maneeprakorn and P. Winotai, *Thermochim. Acta*, **447**, 115 (2006); <https://doi.org/10.1016/j.tca.2006.04.013>.
- A.R. Boyd, L. Rutledge, L.D. Randolph and B.J. Meenan, *Mater. Sci. Eng. C*, **46**, 290 (2015); <https://doi.org/10.1016/j.msec.2014.10.046>.
- B. Tian, W. Chen, Y. Dong, J.V. Marymont, Y. Lei, Q. Ke, Y. Guo and Z. Zhu, *RSC Adv.*, **6**, 8549 (2016); <https://doi.org/10.1039/C5RA25391H>.
- P. Wang, C. Li, H. Gong, X. Jiang, H. Wang and K. Li, *Powder Technol.*, **203**, 315 (2010); <https://doi.org/10.1016/j.powtec.2010.05.023>.
- N. Specchia, A. Pagnotta, M. Cappella, A. Tampieri and F. Greco, *J. Mater. Sci.*, **37**, 577 (2002); <https://doi.org/10.1023/A:1013725809480>.
- B. Singh, A.K. Dubey, S. Kumar, N. Saha, B. Basu and R. Gupta, *Mater. Sci. Eng. C*, **31**, 1320 (2011); <https://doi.org/10.1016/j.msec.2011.04.015>.
- L. Argueta-Figueroa, R.A. Morales-Luckie, R.J. Scougall-Vilchis and O.F. Olea-Mejía, *Progr. Nat. Sci.: Materi. Int.*, **24**, 321 (2014); <https://doi.org/10.1016/j.pnsc.2014.07.002>.
- C.P. Dhanalakshmi, L. Vijayalakshmi and V. Narayanan, *Asian J. Chem.*, **24**, 5497 (2012).
- V. Stanic, D. Janackovic, S. Dimitrijevic, S.B. Tanaskovic, M. Mitric, M.S. Pavlovic, A. Krstic, D. Jovanovic and S. Raiëvic, *Appl. Surf. Sci.*, **257**, 4510 (2011); <https://doi.org/10.1016/j.apsusc.2010.12.113>.
- K.P. Tank, K.S. Chudasama, V.S. Thaker and M.J. Joshi, *J. Cryst. Growth*, **401**, 474 (2014); <https://doi.org/10.1016/j.jcrysgro.2014.01.062>.